euronoise

A half-space BEM for the simulation of sound propagation above an impedance plane

Haike Brick[a] and Martin Ochmann[b]

[a]TFH Berlin - University of Applied Sciences, FB II, Mathematics - Physics - Chemistry, Luxemburger Str. 10, 13353 Berlin, Germany
[b]Technische Fachhochschule Berlin, Univ. of Applied Sciences, Luxemburger Str. 10, 13353 Berlin, Germany
brick@tfh-berlin.de

The Boundary-Element-Method is a powerful tool for the simulation of sound radiation and scattering. Classically, it was developed for the free 3D-space, but it can be modified easily for half-space solutions as long as the half-space is delimited by a perfectly rigid or soft plane. In this case, the Green's function, the core of the BEM, can be derived from a simple image source ansatz, which however cannot be used for a more general impedance boundary condition. In this presentation, an appropriate Green's function will be studied, which is able to describe the sound propagation above an impedance plane and is suitable for an implementation into a BEM code. It bases on the superposition of sound sources with complex source points. The numerical evaluation of this Green's function will be presented along with several test cases. The computational costs of the developed "Complex-Source-Point-BEM" (CBEM) in comparison with a classical BEM together with a discretisation of the impedance plane will be discussed.

1 Introduction

The purpose of the present work is to calculate the sound field, which is radiated by a vibrating structure in presence of an infinite plane, which is characterized by its normal impedance. The boundary element method (BEM) is well suited for the calculation of the sound radiation of complex structures, but the presence of an impedance plane represents a serious difficulty for the application of the BEM. The infinite plane can be approximated by an additional discretized structure. Apart from the low accuracy, which can be gained with this approach, the supplementary structure enlarges the set of equations considerably. Another way is to incorporate an appropriate Green's function into the BEM formulation, which fulfills the boundary conditions on the impedance plane automatically. In literature there can be found numerous solutions for the Green's function describing the sound propagation above an impedance plane, e.g. [1], [2], [3]. Unfortunately, all those solutions have singularities for an impedance with springlike reactance and special source-receiver geometries. They are not suited for an implementation in a BEM code for the simulation of outdoor sound propagation, since most of real ground surfaces show springlike impedance characteristics [4]. Also, in [5], which directly focuses on the BEM, a sufficient solution for this configuration could not be found. Ochmann presented in [6] a Green's function, which seems suitable for an incorporation into a BEM code, since it does not have any limitations considering the impedance characteristics of the plane or the placement of source and receiver. In the following work this Green's function and its implementation in a BEM code will be discussed. At first a brief survey of the theoretical background will be given, followed by details about the numerical implementation of the function. Two test cases will be presented to verify the implementation. The paper concludes with a investigation of the accuracy and effectiveness of the new CBEM formulation in comparison with an indirect BEM and a discretized impedance plane.

2 Theory

The basis for the BEM is the Helmholtz-Integral-Equation (HIE), here for exterior problems,

$$C(\vec{x})p(\vec{x}) = \int_{S_Q} \left(p(\vec{y}) \frac{\partial g(\vec{x},\vec{y})}{\partial \vec{n}_y} - \frac{\partial p(\vec{y})}{\partial \vec{n}_y} g(\vec{x},\vec{y}) \right) dS_y \tag{1}$$

with

$$C(\vec{y}) = \begin{cases} 1 & \vec{x} \text{ in the exterior domain,} \\ \frac{1}{2} & \vec{x} \text{ on the surface } S_Q, \\ 0 & \vec{x} \text{ in the interior domain.} \end{cases}$$

The core of the HIE is the Green's function $g(\vec{x},\vec{y})$. As solution of the wave equation it describes the sound propagation between the source point $\vec{y} = (x_s,\, y_s,\, z_s)$ and the receiver point $\vec{x} = (x,\, y,\, z)$ and has to fulfill the boundary condition on the surface as well as Sommerfelds radiation condition at infinity. For the free-space case the Greens function is given by

$$g(\vec{x},\vec{y}) = \frac{e^{-\mathrm{i}kR_1}}{4\pi R_1} \tag{2}$$

with $R_1 = \sqrt{(x-x_s)^2 + (y-y_s)^2 + (z-z_s)^2}$. k is the wavenumber $k = \omega/c_0$ with ω as angular frequency and c_0 the speed of sound in the acoustic domain. The time dependence $\exp(\mathrm{i}\omega t)$ is omitted.

Regarding a half-space problem, the three-dimensional space is separated by an infinite plane S_p, see Fig. 1. The boundary condition on the plane is given by the plane's normal impedance Z

$$\frac{p}{v_n} = Z \quad \text{on } S_p. \tag{3}$$

As long as the $Z = \infty$ or $Z = 0$, which corresponds to a perfectly rigid and soft plane, respectively, the appropriate Green's function is given by an image source ansatz

$$g(\vec{x},\vec{y}) = \frac{e^{-\mathrm{i}kR_1}}{4\pi R_1} + R_p \frac{e^{-\mathrm{i}kR_2}}{4\pi R_2} \tag{4}$$

with

$$R_p = \begin{cases} +1 & Z = \infty, \\ -1 & Z = 0. \end{cases} \tag{5}$$

In [6] a Green's function was presented, which are able to fulfill any impedance boundary condition on the plane S_p and has no restrictions relating to the position of $\vec{x}$ and $\vec{y}$

$$G(\vec{x},\vec{y}) = \frac{e^{-\mathrm{i}kR_1}}{4\pi R_1} + \frac{e^{-\mathrm{i}kR_2}}{4\pi R_2} + \frac{\mathrm{i}\gamma}{2\pi} \int_{-\infty}^{0} \underbrace{\frac{e^{-\mathrm{i}k\sqrt{\rho^2 + (z+z_s+\mathrm{i}\zeta)^2}}}{\sqrt{\rho^2 + (z+z_s+\mathrm{i}\zeta)^2}}}_{\hat{g}(-z_s-\mathrm{i}\zeta)} e^{-\mathrm{i}\gamma\zeta} \mathrm{d}\zeta, \tag{6}$$

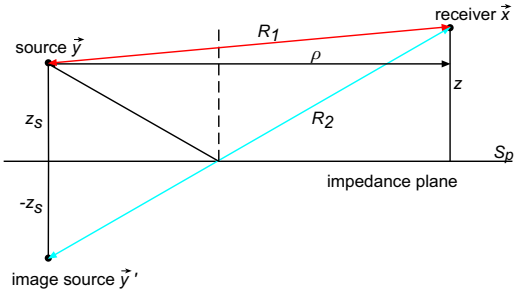

Figure 1: Sketch of source $\vec{y}$ and receiver $\vec{x}$ above an infinite plane

where $\rho = \sqrt{(x-x_s)^2 + (y-y_s)^2}$ is the horizontal distance between $\vec{x}$ and $\vec{y}$. γ follows from the plane's normalized impedance, $\gamma = \mathrm{i}k/Z_0$ mit $Z_0 = Z/(\rho_0 c_0)$ with $\rho_0 c_0$ as impedance of the ambient fluid. The integral in (6) can be interpreted as line integral over image sources with a complex source point, $\hat{g}(-z_s - \mathrm{i}\zeta)$. A more detailed presentation of the theoretical background of (6) and its derivation and the characteristics of point sources with complex source points can be found in [6] and [7]. Eq. (6) does not have any singularities, apart from grazing incidence when $z + z_s = 0$, i.e. source and receiver position must not be directly located on the plane. The integral is convergent for masslike and springlike reactive parts of the plane impedance. Its drawback is that it is an improper integral over a fluctuating kernel, which can show a narrow peak at $\zeta = -\rho$.

3 Numerical Evaluation

Due to the difficult kernel in the integral of Eq. (6) an evaluation of the integral can be quite tedious. A very reliable method is the adaptive multigrid quadrature, which is presented in [8]. This quadrature method requires the determination of a lower integration limit. The integrand $\Psi(\zeta)$ can be separated into a decaying envelope $\Psi_E(\zeta)$ and a oscillating term $\Psi_O(\zeta)$

$$\begin{aligned}\Psi(\zeta) =& \frac{e^{-\mathrm{i}kr}}{r}\, e^{-\mathrm{i}\gamma\varsigma} \\ =& \underbrace{1/|r|\, e^{(k\,\mathrm{Im}\{r\}+\mathrm{Im}\{\gamma\}\zeta)}}_{\Psi_E(\zeta)} \underbrace{e^{-\mathrm{i}(k\,\mathrm{Re}\{r\}+\phi+\mathrm{Re}\{\gamma\}\zeta)}}_{\Psi_O(\zeta)}\end{aligned} \tag{7}$$

with $r = \sqrt{\rho^2 + (z + z_s - \mathrm{i}\zeta)^2}$. Re{ } and Im{ } denote the real and imaginary part of the quantity in brackets, respectively. Since Im{γ} represents the damping of the ground, Im{γ} must be equal or greater than zero and the exponent in $\Psi_E(\zeta)$ is negative for all $\zeta \in (-\infty, 0]$. This decaying envelope ensures the convergence of the integral in (6) on one hand and it provides the possibility of defining a lower limit on the other. We decide to terminate the integration at ζ_{ll} where $\Psi_E(\zeta) < 10^{-6}$. Fig. 2 shows the kernel of the integral and the components of the envelope $\Psi_E(\zeta)$ for $z + z_s \ll 0$, i.e. for $\vec{x}$ and $\vec{y}$ close to the plane. For the implementation of the quadrature algorithm the program package "mlquad" from "CodeLib" was used and the code was adapted to

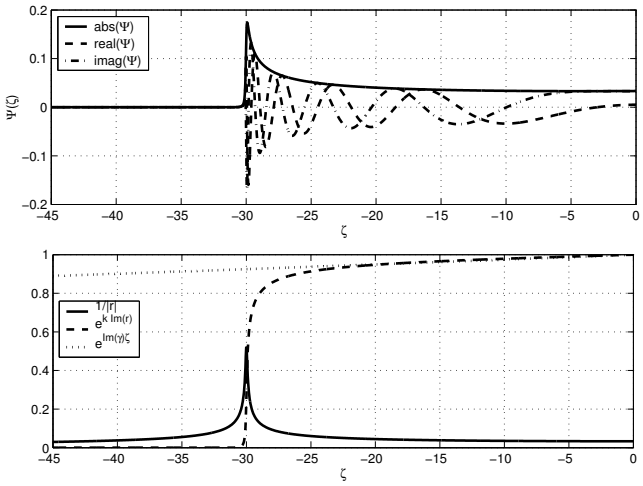

Figure 2: *Upper panel*: Curve of $\Psi(\zeta)$ in case $z + z_s << 1$ for $\rho = 30$ m, $\gamma = 0.0026 + \mathrm{i}0.0026$ m^{-1}, $z + z_s = 0.06$ m, $k = 1$ m^{-1}. *Lower panel*: Components of the envelope $\Psi_E(\zeta)$.

the present integral. "CodeLib" is a collection of algorithms of the Konrad-Zuse-Zentrum für Informationstechnik Berlin [9].

In case Im{γ} > 1, the Gauss-Laguerre quadrature can be applied to solve the integral in (6). This leads to an enormous acceleration of the calculation. The Gauss-Laguerre quadrature is defined as

$$\int_0^\infty f(\eta) e^{-\eta} \mathrm{d}\eta = \sum_{i=1}^{n} w(i) f(\eta(i)). \tag{8}$$

By means of a variable transformation with $\eta = -\zeta\,\mathrm{Im}\{\gamma\}$ the integral in (6) can be converted into the appropriate form,

$$I = \frac{\mathrm{i}\gamma}{2\pi\,\mathrm{Im}\{\gamma\}} \int_0^\infty \underbrace{\frac{e^{-\mathrm{i}k\widetilde{r}}}{\widetilde{r}} e^{\mathrm{i}\eta\,\mathrm{Re}\{\gamma\}/\,\mathrm{Im}\{\gamma\}}}_{f(\eta)} e^{-\eta} \mathrm{d}\eta \tag{9}$$

with $\widetilde{r} = \sqrt{\rho^2 + (z + z_s - \mathrm{i}\eta/\,\mathrm{Im}\{\gamma\})^2}$. The number of quadrature points n depends on the curve of the integral kernel. Our investigations showed, that the sum of the heights of source and receiver location has the most influence on the necessary number n. The closer source and receiver are located to the plane, the more quadrature points are necessary to solve the integral correctly.

The expression for $f(\eta)$ contains also an exponentially decaying term, namely $\exp(k\,\mathrm{Im}\{\widetilde{r}\})$. In case the decay of the term $\exp(k\,\mathrm{Im}\{\widetilde{r}\})$ is considerably more steep as the decay of $\exp(-\eta)$, the integral can not be solved by the Gauss-Laguerre quadrature. From this it follows that this quadrature formula can only be applied for Im{γ} > 1. However, in this case the Gauss-Laguerre quadrature is observed to solve the integral correctly and very fast. A resistance of Im{γ} > 1 can be found for soft grounds in the higher frequency range.

4 Test cases

4.1 Soft ground

The test configuration is given by a small cube with edge length of 1 m, whose surface is driven by a virtual monopole source in its center [10], [11]. The surface mesh consists of 54 four-noded quadrilateral elements. The center of the cube is located 3 m above the infinite impedance plane, which is located in $z = 0$, see Fig. 3. The perfectly soft plane impedance is approximated by a very high admittance of $|\gamma| = \sqrt{2}\cdot 10^{-3}$. Both a masslike ($\mathrm{Re}\{\gamma\} > 0$) and a springlike ($\mathrm{Re}\{\gamma\} < 0$) plane impedance are investigated. Fig. 3 shows the BEM results for the sound pressure in field points in a distance of 3 m around the center of the cube, see Fig. 3, for the image-source Green's function BEM (IMBEM), Eq. (4), and the complex Green's function BEM (CBEM), Eq. (6). The sound pressure was normalized to $\rho_0 c|\bar{v_n}|$, with $|\bar{v_n}|$ as absolute value of the mean surface velocity of the pulsating object. For the illustrated benchmark configuration the results of the CBEM formulation match very well the results of the IMBEM.

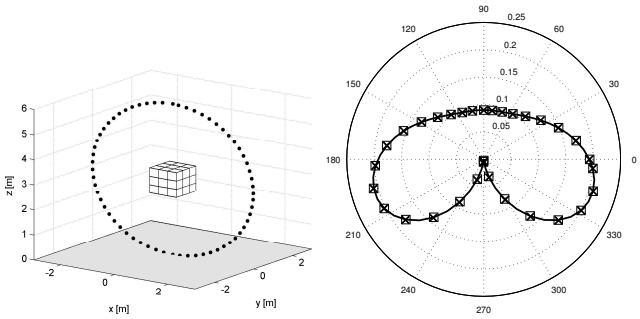

Figure 3: *Left panel*: Test geometry: Field points around the radiating cube above an impedance plane. *Right panel*: Normalized sound pressure in the field points: — calculated with IMBEM in case of a perfectly soft plane ($R_p = -1$); □ calculated with the CBEM for a soft plane with masslike impedance ($\gamma = 10^3 + \mathrm{i}10^3$ m^{-1}) and × for a soft plane with springlike impedance ($\gamma = -10^3 + \mathrm{i}10^3$ m^{-1})

4.2 Perpendicular incidence

In case, source and receiver are arranged one above the other on a vertical axis ($\rho = 0$), there exists a exact solution for Eq. (6)

$$G_{\mathrm{exakt}}(\vec{x},\vec{y}) = \frac{e^{-\mathrm{i}kR_1}}{4\pi R_1} + \frac{e^{-\mathrm{i}kR_2}}{4\pi R_2} - \frac{\mathrm{i}k}{2\pi Z_0} e^{\mathrm{i}k\,(z+z_s)/Z_0} E_1\left(\mathrm{i}k\,(z+z_s)\left(1+\frac{1}{Z_0}\right)\right). \tag{10}$$

For field points far above the impedance plane, where $k(z+z_s)$ is large, Eq. (10) can be simplified to a "plane wave"-approximation [12]

$$G_{\mathrm{plane}}(\vec{x},\vec{y}) = \frac{e^{-\mathrm{i}kR_1}}{4\pi R_1} + \frac{Z_0 - 1}{Z_0 + 1}\frac{e^{-\mathrm{i}kR_2}}{4\pi R_2}. \tag{11}$$

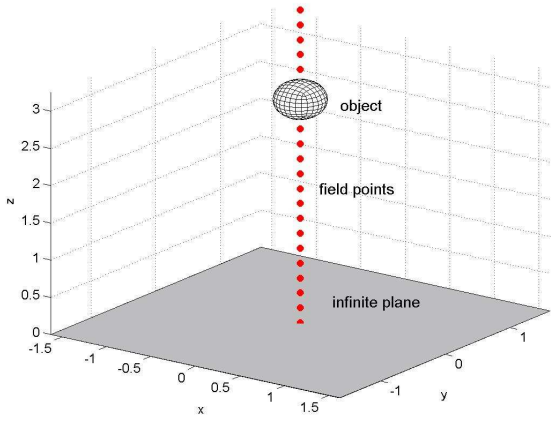

Figure 4: Vibrating sphere above an impedance plane, the field points are located on a vertical line at $x_{\mathrm{FP}} = (0,\, 0,\, z)$

The geometry of the test configuration can be seen in Fig. 4. A sphere of radius 0.25 m is located above an impedance plane with $\gamma = 1 + 0.5\,\mathrm{i}$. The sphere's center is located at (0, 0, 3m), the wave number is $k = 1$ m^{-1}. The sphere's surface is build up by 296 quadrilateral and triangular elements. The field points are arranged on a vertical line below and above the sphere's center at $\vec{x}_{\mathrm{FP}} = (0,\, 0,\, z)$. The sphere vibrates with a normal velocity distribution, which is determined by a virtual monopole source in the center of the sphere at $\vec{y}$. Due to the presence of the impedance plane the velocity v_n is not uniform, but can be obtained by means of Eq. (6). Thus, the normal velocity v_n of the nodes $\vec{x}$ of the sphere are given by

$$v_n(\vec{x}) = \frac{\mathrm{i}}{\omega\rho_0} A_p \frac{\partial G(\vec{x},\vec{y})}{\partial \vec{n}_x}. \tag{12}$$

A_p is the source strength of the virtual monopole source in the interior of the sphere.

From Gl. (10) follows the exact sound pressure at the field points p_{exact}. The error E is a measure for the deviation of the field point sound pressure from the exact solution

$$E_i = \sqrt{\frac{|p_i - p_{\mathrm{exakt}}|^2}{|p_{\mathrm{exakt}}|^2}}, \tag{13}$$

with p_i as sound pressure at the field points coming from the "plane wave"-approximation and the CBEM-solution. Fig. 5 shows the error curves. The error of the monopole test E_{disc} is additionally plotted. E_{disc} represents the general discretization error of the numerical solution, as it was decribed in [10]. It can be seen, that the error of the CBEM-solution E_{CBEM} is in the order of magnitude of the discretization error at around 1%. As expected, the error of the "plane wave"-approximation is very high for field points in proximity to the plane. For field points at larger z, the error decreases and the approximation converges to the exact solution. This test verifies the implementation of the Green's function (6) into the BEM-application and shows, that the CBEM is able to approximate excellently the radiated sound field above an impedance plane.

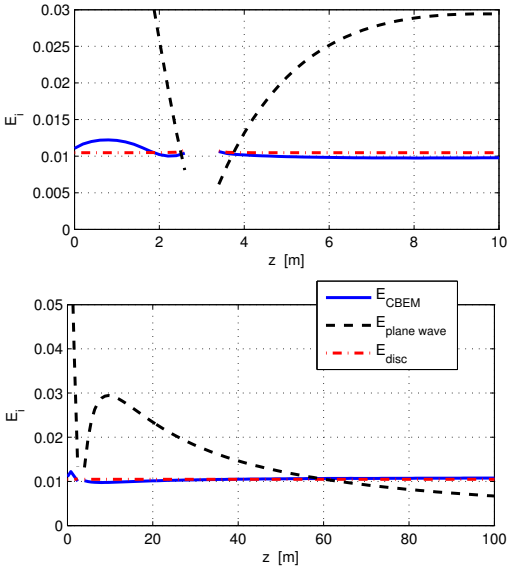

Figure 5: Error E of the "plane wave"-approximation and of CBEM-solution as well as the discretization error

5 Application of the CBEM

In a first step we investigate the accuracy of the the multigrid quadrature and the Gauss-Laguerre quadrature within a CBEM simulation and later on we compare the CBEM results to results of an indirect BEM, where the infinite impedance plane is represented by a discretized plane model.

The geometrical configuration can be found in Fig. 6. The center of the vibrating sphere, which was already introduced in Sec. 4.2, is now located at (0, 0, 1m) above the impedance plane with $\gamma = -1.41 + \mathrm{i}\,1.66$ at $f = 400$ Hz (forest floor). 100 field points are located on a horizontal line at $\vec{x}_{\mathrm{FP}} = ([0.5 : 300]\mathrm{m}, 0, 1\mathrm{m})$. Fig. 7

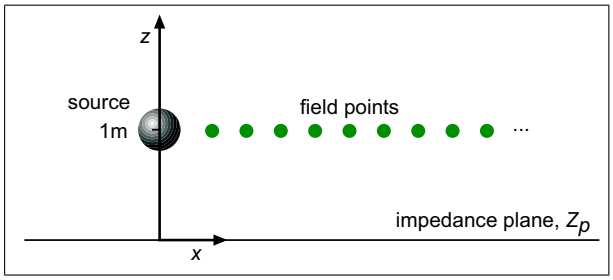

Figure 6: Vibrating sphere above an impedance plane, the field points are located on a horizontal line at $\vec{x}_{\mathrm{FP}} = (x, 0, 1\mathrm{m})$

shows the error E, Eq. (13), of the CBEM-solution for this configuation calculated with the multigrid quadrature $E_{\text{CBEM-mlquad}}$ and the Gauss-Laguerre quadrature $E_{\text{CBEM-GL}}$, respectively. Here, p_{exact} is the field points pressure, calculated with Eq. (6) by means of a multigrid quadrature of the integral term. The discretization error E_{disc} is additionally plotted. Again, the error of both CBEM-solutions, $E_{\text{CBEM-GL}}$ and $E_{\text{CBEM-mlquad}}$, is in the order of magnitude of the discretization error of 2.5 % over a wide range of the horizontal distance x. At very far distances, for $kx > 400$ some peak-shaped deviations from this error level occur. The cause of this deviations could not be ascertained so far. It seems, that there occur numerical instabilities for some selected geometrical configuations, provided that the field points are very far away from the source.

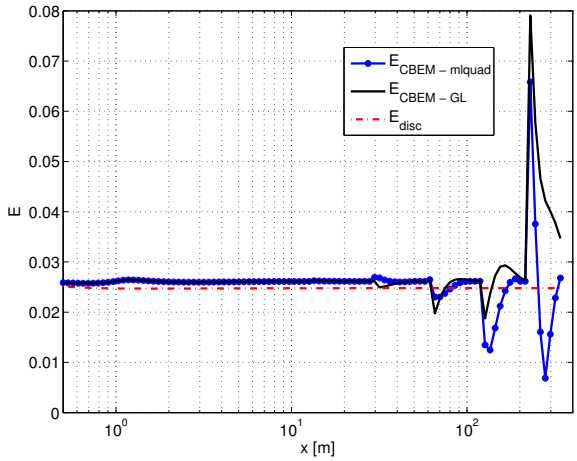

Figure 7: Error of the CBEM-solution with multigrid quadratrure $E_{\text{CBEM-mlquad}}$ and with Gauss-Lagurerre quadrature $E_{\text{CBEM-GL}}$ as well as the discretization error E_{disc}

In the next step, the impedance plane in Fig. 6 is represented by a set of planar quadrilateral elements, see Fig. 8. We investigate two measures of the discretized plane, 6×6 m with 2304 elements and 12×12 m with 9216 elements. Since the plane does not have a closed surface the indirect BEM has been used. The calculation was carried out with LMS Virtual.Lab Rev.7B. Fig. 9 shows the error of the field points pressure for the two planes in comparison with the previously discussed $E_{\text{CBEM-GL}}$. It can be clearly seen, that outside the discretized plane areas the error becomes huge (the edges of the planes are indicated by the arrows, labeled with 3m and 6m). With increasing x the sound field becomes more and more the sound field of an monopole source in free space, therefore the enormous deviations from the exact solution occur at the outlying field points. But also at the field points above the plane model a large error is detected, even near the middle of the planes. The increased edge length of the greater plane does not enhance the results much. The error curves show, that the CBEM simulates the radiated sound field above an impedance plane with a very high grade of accuracy, which can not be reached by using a discretized plane model. The cost for the different simulation approaches

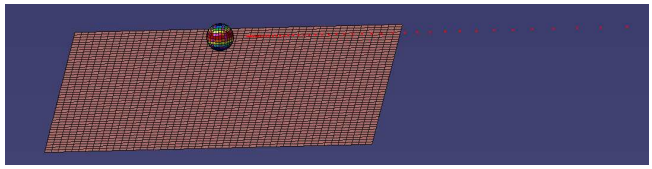

Figure 8: Vibrating sphere above a discretized impedance plane

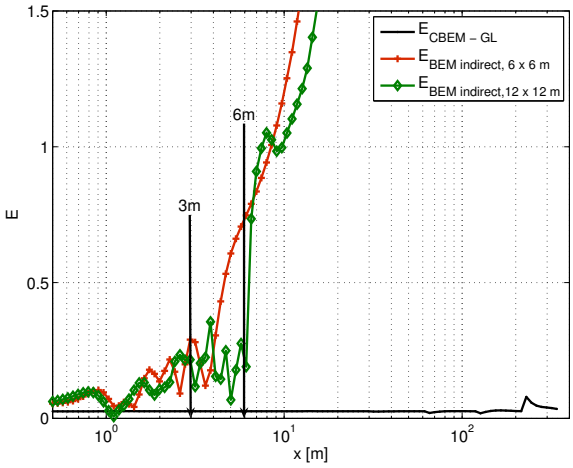

Figure 9: Error of the sound pressure at the field points for the different simulations

can be found in Tab. 1. All calculations were done on a desktop PC with Intel Pentium D Dualcore, running at 3.20 GHz, equipped with 2.00 GB RAM, OS Windows XP. BemLab is our in-house Matlab-based BEM code, described in [7], [13]. The multigrid quadrature

Method	Software	Time needed
Cbem-mlquad	BemLab	4 h
Cbem-GL	BemLab	0.5 min
indirect Bem, 6×6m	Virtual.Lab	5 min
indirect Bem, 12×12m	Virtual.Lab	1.5 h

Table 1: Costs for the different simulation methods

(Cbem-mlquad) of the integral term of Eq. (6) has comparatively high costs. At present the Cbem in combination with a Gauss-Laguerre quadrature (Cbem-GL) is the most favorable approach regarding quality and speed of the Bem-calculation.

6 Summary

A Green's function, which describes the sound propagation above an impedance plane, was successfully implemented in a Bem-code. Due to the characteristics of the Greens' function there does not exist any limitation for the applicability of the resulting Cbem. Hence, the impedance planes are allowed with masslike as well as springlike reactive parts. All arrangements of source and receiver points are possible. It could be shown, that the quality of the Cbem-solution is much higher than of a comparable indirect Bem-model. Thus, the presented Cbem represents a very valuable extension of the classical Bem-formulation for the description of more realistic models considering outdoor sound propagation.

References

[1] K. Attenborough, S. I. Hayek, and J. M. Lawther. Propagation of sound above a porous half-space. *J. Acoust. Soc. Am.*, 68(5):1493–1501, 1980.

[2] S-I. Thomasson. Asymptotic solution for sound propagation above an impedance boundary. *Acustica*, 45:122–125, 1980.

[3] D. Habault and P. J. T. Filippi. Ground effect analysis: Surface wave and layer potential representations. *Journal of Sound and Vibration*, 79(4):529–550, 1981.

[4] M. Ögren and H. Jonasson. *Measurement of the Acoustic Impedance of Ground*. SP Swedisch National Testing and Research Institut, SP Report 1998:28, 1998.

[5] W. L. Li, T. W. Wu, and A. F. Seybert. A half-space boundary element method for acoustic problems with a reflecting plane of arbitrary impedance. *Journal of Sound and Vibration*, 171(2):173–184, 1994.

[6] M. Ochmann. The complex equivalent source method for sound propagation over an impedance plane. *J. Acoust. Soc. Am.*, 116(6):3304–3311, 2004.

[7] M. Ochmann and H. Brick. Acoustical radiation and scattering above an impedance plane. In S. Marburg and B. Nolte, editors, *Computational Acoustics of Noise Propagation in Fluids. Finite and Boundary Element Methods*, chapter 17, pages 459–494. Springer Verlag, Berlin, 2008.

[8] P. Deuflhard and A. Hohmann. *Numerische Mathematik I - Eine algorithmisch orientierte Einführung*, chapter 9.7, pages 343–351. de Gruyter, Berlin, New York, 1993.

[9] P. Deuflhard and A. Hohmann. Numerical analysis and modelling–CodeLib. `http://www.zib.de/Numerik/numsoft/CodeLib`.

[10] M. Ochmann and A. V. Osetrov. Construction of analytical solutions for the error estimation of acoustical boundary element solvers. In *Proc. of the Forum Acusticum*, pages 1000–1004, Sevilla, 2002.

[11] A. V. Osetrov and M. Ochmann. A fast and stable numerical solution for acoustic boundary element method equations combined with the Burton and Miller method for models consisting of constant elements. *Journal of Computational Acoustics*, 13(1):1–20, 2005.

[12] M. A. Nobile and S. I. Hayek. Acoustic propagation over an impedance plane. *J. Acoust. Soc. Am.*, 78(4):1325–1336, 1985.

[13] H. Brick, M. Ochmann, and E. Brenck. Simulation of the sound radiation from wheel-like structures using the boundary element method. *Forum Acusticum, Sevilla*, 2002.